2219 Applied Optics
34(1995)10 March, No.8, Washington, DC, US

Visor-display design based on planar holographic optics

Y. Amitai, S. Reinhorn, and A. A. Friesem

A method for designing and recording visor displays based on planar holographic optics is presented. This method can deal with the problem of recording-readout wavelength shift. The display system is composed of two holographic optical elements that are recorded on the same substrate. One element collimates the waves from each data point in the display into a plane wave that is trapped inside the substrate by total internal reflection. The other diffracts the plane waves into the eye of an observer. Because the chromatic dispersion of the first element can be corrected by the dispersion of the second, this configuration is relatively insensitive to source wavelength shifts. The method is illustrated by the design, recording, and testing of a compact holographic doublet visor display. The recording was at a wavelength of 458 nm, and readout was at 633 nm. The results indicate that diffraction-limited performance and relatively low chromatic dispersion over a wide field of view can be obtained.

Key words: Planar optics, optical design, displays, holography.

1. Introduction

One of the important applications for holographic optical elements (HOE's) is in visor displays; a HOE serves as an imaging lens and a combiner, where a two-dimensional quasi-monochromatic display is imaged to infinity and reflected into an observer's eye. The display can be derived either directly from a CRT or indirectly by means of a relay lens or an optical fiber bundle. Typically the display is composed of an array of points whose geometry at readout differs from that at recording. As a result, the imaged array contains aberrations that decrease the image quality. In addition, it is often necessary to record the HOE's at a wavelength that differs from the readout wavelength. This is particularly true when the readout wavelength is not suitable for recording the HOE's. Such a wavelength shift introduces additional aberrations. Another problem, which is usually common to all types of diffractive optical elements, is their relatively high chromatic dispersion. This is a major drawback in applications where the light source is a CRT that is not purely monochromatic. Recently several new designs were proposed for improving the performance of holographic lenses.[1–7] These designs, which deal only with single HOE's, compensate for the geometric and chromatic aberrations by using nonspherical waves rather than simple spherical waves for recording. However, they do not overcome the chromatic dispersion problem.

In this paper we present a method for designing and recording HOE's for visor displays in which both the aberrations and the chromatic dispersions are minimized. In this method, planar (substrate-mode[8–10]) optics schemes are exploited for recording a holographic doublet visor display (HDVD), composed of a corrected collimating lens and a simple linear grating. The lens collimates the light from the input display to form an array of plane waves, and it diffracts these plane waves so that they will be trapped inside the substrate. The grating merely diffracts the trapped light outward. In order to achieve low aberrations, one records the collimating lens with predistorted waves that are derived recursively from holograms recorded with spherical waves and whose readout geometries differ from those used during recording. An inherent advantage of these HDVD's is that they can be incorporated into relatively compact systems. Our method is illustrated by the design and recording of a compact HDVD. The recording was at a wavelength of 458 nm, and the readout was at 633 nm. The results reveal that an HDVD can handle a field of view (FOV) of ±6° with essentially diffraction-limited performance, and low chromatic sensitivity can be readily achieved.

The authors are with the Department of Physics of Complex Systems, Weizmann Institute of Science, Rehovot 76100, Israel.

Y. Amitai is now mainly with the optronic products division, Electro-optics Industries LTD, P.O. Box 1165, Rehovot 76111, Israel.

Received 7 March 1994; revised manuscript received 28 [illegible] 1994

0003-6935/95/081352-05$06.00/0

2. Design Consideration

The readout geometry for the HDVD is schematically presented in Fig. 1. The doublet is composed of two holographic elements, a collimating lens $\mathcal{H}_d$ and a simple linear grating $\mathcal{H}_g$, both of which are recorded on the same substrate. A two-dimensional display is located at a distance R_d from the center of $\mathcal{H}_d$, where R_d is the focal length of $\mathcal{H}_d$. The light from the displays is thus transformed into an angular spectrum of planar wave fronts by $\mathcal{H}_d$. Specifically, each viewing angle of the input is diffracted into a plane wave at an angle $\bar{\beta}_i^d(x)$ inside the substrate, where x is the lateral coordinate of $\mathcal{H}_d$. So that the image waves will be trapped inside the plate by total internal reflection, $\bar{\beta}_i^d(x)$ must satisfy the relation

$$\nu \geq \sin \beta_i^d(x) \equiv \nu \sin \bar{\beta}_i^d(x) \geq 1, \tag{1}$$

where ν is the refractive index of the glass plate. The linear grating $\mathcal{H}_g$ diffracts the trapped wave fronts outward. An observer located at a distance R_{eye} would thus see an image of the display located at infinity. In reality the light rays emerging from the display are collected and imaged by the HDVD onto the observer's eye. Nevertheless, it is more convenient to analyze the aberrations caused by the HDVD by inversion of the direction of the light rays. Thus the readout waves of $\mathcal{H}_g$ form an angular spectrum of plane waves (each having the diameter of the eye's pupil d_{eye}) that emerge from the eye and are focused by the HDVD onto the display plane. The central wave is focused to the center of the display, whereas the foci of the other waves are laterally displaced.

The design of the linear grating $\mathcal{H}_g$ is straightforward. It has a grating function $H_g = (2\pi/\lambda_c)(\nu \sin \bar{\beta}_i^g)\xi$, where λ_c is the readout wavelength, ξ is the lateral coordinate of $\mathcal{H}_g$, and $\bar{\beta}_i^g(0) = \bar{\beta}_i^d(0)$ is the off-axis angle of the central ray inside the substrate.

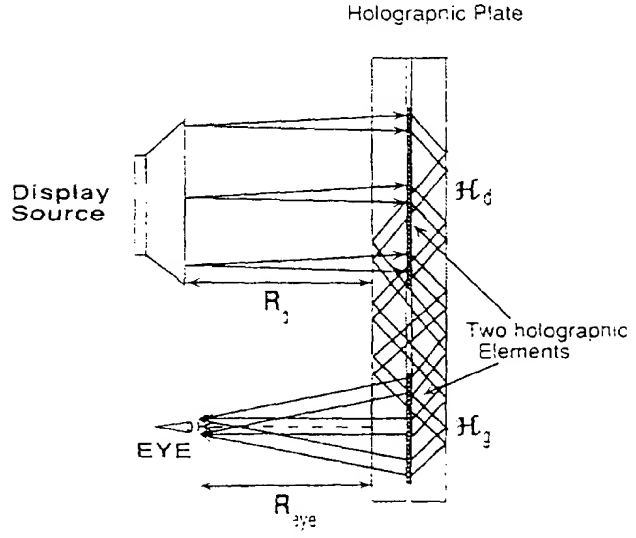

Fig. 1. Readout geometry of the planar-optics holographic doublet visor display

The design of the collimating lens $\mathcal{H}_d$ is much more complicated, so we concentrate on it.

We begin with the basic relations[3] for a simple holographic imagery lens recorded with spherical waves, given as

$$\mu\left(\frac{1}{R_o} - \frac{1}{R_r}\right) = \frac{1}{R_d},$$

$$\mu_r(\sin \beta_x - \sin \beta_{ox}) = \sin \beta_{cx}, \tag{2}$$

where c, o, and r are the indices for the reconstruction, object, and reference waves, respectively, R_q ($q = o, r$) is the distance between the respective point source and the center of the hologram, β_{qx} ($q = o, r$) is the respective off-axis angle, β_{cx} is defined as $\beta_{cx} \equiv \nu\bar{\beta}_{cx} = \nu\bar{\beta}_i^g(0)$, and μ is the ratio between the readout and the recording wavelengths (i.e., $\mu = \lambda_c/\lambda_r$). Unfortunately, a simpler holographic lens, recorded with spherical waves only, in general has large aberrations over the entire FOV. In order to compensate for the large aberrations, we need to record the holographic lens with two aspherical waves.

3. Exploiting the Recursive Design Method

There are several methods[3,4,11] for designing and recording holographic imaging lenses with low aberrations as needed. We chose the recursive design technique[4] because the recording procedure is relatively simple and there is no need to resort to computer-generated holograms that require sophisticated recording equipment.

In this recursive design and recording method, aspheric wave fronts for recording the final collimating lens are derived from interim holograms. Specifically the aspheric object and reference waves are derived from intermediate holograms $\mathcal{H}^o$ and $\mathcal{H}^r$, respectively (the superscript o will denote all the parameters that are related to $\mathcal{H}^o$, and the superscript r will denote the parameters related to $\mathcal{H}^r$).

To avoid large astigmatism and coma in the center of the FOV, we must record the $\mathcal{H}_d$ with a combination of plane waves and on-axis spherical waves.[4] We now let the reference waves of $\mathcal{H}^o$ and $\mathcal{H}^r$ be plane waves, i.e., $R_r^o = R_r^r = \infty$. We also let the object and the reconstruction waves of $\mathcal{H}^o$ and $\mathcal{H}^r$ be spherical waves normal to the hologram plane; i.e., $\sin \beta_x^o = \sin \beta_{ox}^o = \sin \beta_{ox}^r = \sin \beta_{cx}^r = 0$. Thus the imaging equations are rewritten as

$$\mu\left(\frac{1}{R_o^o} + \frac{1}{R_c^o} - \frac{1}{R_o^r} - \frac{1}{R_c^r}\right) = \frac{1}{R_d},$$

$$\mu_r(\sin \beta_c^o - \sin \beta_o^r) = \sin \beta_{cx}. \tag{3}$$

It is apparent from Fig. 1 that a single plane wave, representing a particular viewing angle, focused by $\mathcal{H}_g$ to a point in the output plane, illuminates only part of the overall hologram. Thus we may define for each viewing angle a local hologram whose aberrations must be determined and minimized. Let us consider the local hologram at a distance x from the center of the overall hologram. We denote the rel-

evant parameters for the overall hologram as R_q^o, β_q^o, and those for the local hologram as $R_q^o(x)$, $\beta_q^o(x)$, where $q = o, c$ and $p = o, r$. Under the assumption of small angles, the parameters of the interim holograms are

$$\sin \beta_q^o(x) \approx \frac{x}{R_q^o} - \frac{1}{2}\frac{x^3}{(R_q^o)^3}, \tag{4}$$

$$R_q^o(x) = \frac{R_q^o}{\cos \beta_q^o(x)} \approx \frac{R_q^o}{1 - 1/2 \sin^2 \beta_q^o(x)} \approx \frac{R_q^o}{1 - 1/2(x/R_q^o)^2 + 1/2(x/R_q^o)^4}, \tag{5}$$

$$\sin \beta_c^o(x) = \sin \beta_c^o. \tag{6}$$

When $\Delta\bar{\beta}_c$ is sufficiently small, we may write

$$\sin \bar{\beta}_c(x) = \sin(\bar{\beta}_c + \Delta\bar{\beta}_c) = \sin \bar{\beta}_c + \Delta\bar{\beta}_c \cos \beta_c. \tag{7}$$

By use of the holographic imaging equation it is possible to derive[4]

$$\sin(\bar{\beta}_c + \Delta\bar{\beta}_c) = \sin \bar{\beta}_c + \frac{\Delta\beta_c^\xi}{\nu} = \sin \bar{\beta}_c + \frac{\xi(x)}{\nu R_{eye}}. \tag{8}$$

Combining Eqs. (7) and (8) yields

$$\Delta\bar{\beta}_c = \frac{\xi(x)}{\nu R_{eye} \cos \bar{\beta}_c}. \tag{9}$$

In accordance with the geometry of Fig. 2 the relation between the lateral coordinate ξ of $\mathscr{H}_g$ and the lateral coordinate x of $\mathscr{H}_d$ is

$$\xi(x) = x - \frac{R_H \Delta\bar{\beta}_c}{\cos \bar{\beta}_c} = x - \frac{R_H \xi(x)}{\nu R_{eye} \cos^2 \bar{\beta}_c}, \tag{10}$$

or

$$\frac{\xi(x)}{\nu R_{eye}} = \frac{x}{\nu R_{eye} + R_H/(\cos^2 \bar{\beta}_c)}, \tag{11}$$

where R_H is the unfolded distance between the center

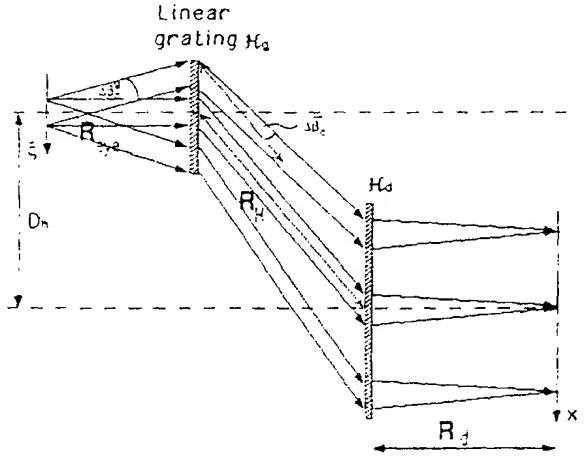

Fig. 2 Unfolded configuration of the holographic doublet.

of the two holograms. Substituting Eq. (11) into Eq. (8) yields

$$\sin \bar{\beta}_c(x) = \sin \bar{\beta}_c + \frac{x}{\nu R_{eye} + R_H/(\cos^2 \bar{\beta}_c)}. \tag{12}$$

With Eqs. (4)–(6) and Eq. (12) it is possible to determine the relevant parameters of the image waves:

$$\begin{aligned}\sin \beta_i(x) &= \nu \sin \bar{\beta}_c(x) + \mu[\sin \beta_c^o - \sin \beta_c^o(x) - \sin \beta_c^o(x) \\ &\quad - \sin \beta_c^r(x) - \sin \beta_c^r(x) + \sin \beta_c^r(x)] \\ &= \sin \beta_c - \frac{x}{R_{eye} + R_H/(\nu \cos^2 \bar{\beta}_c)} \\ &\quad + \mu\left[x\left(\frac{1}{R_c^o} + \frac{1}{R_c^o} - \frac{1}{R_c^r} - \frac{1}{R_c^r}\right) - \sin \beta_c^o + \sin \beta_c^r\right] \\ &= \frac{x}{R_{eye} + R_H/(\nu \cos^2 \bar{\beta}_c)} - \frac{x}{R_d},\end{aligned} \tag{13}$$

where i is the index for the image waves of $\mathscr{H}_i$. Finally, by letting $R_d = R_{eye} - R_H/(\nu \cos^2 \bar{\beta}_c)$, we get the simple result of

$$\sin \beta_i(x) = 0. \tag{14}$$

If the display surface is parallel to the hologram surface, then $R_i(x) = -R_d$. Thus using only the first and the second nonvanishing orders of x, R_q^o in approximations (4) and (5), we obtain the various aberrations of the local hologram. These can be written as

$$\begin{aligned}S(x) &= \frac{-1}{R_i^3(x)} + \mu \sum_{\substack{p=o,r \\ q=c,o}} \epsilon_p \left[\frac{1}{R_q^p(x)}\right]^3 \\ &= \frac{1}{R_d^3} + \mu\left[\sum_{\substack{p=o,r \\ q=c,o}} \epsilon_p \left(\frac{1}{R_q^p}\right)^3 - \frac{3}{2}x^2 \sum_{\substack{p=o,r \\ q=c,o}} \epsilon_p \left(\frac{1}{R_q^p}\right)^5\right],\end{aligned}$$

$$\begin{aligned}C(x) &= \mu \sum_{\substack{p=o,r \\ q=c,o}} \epsilon_p \frac{\sin \beta_q^p(x)}{[R_q^p(x)]^2} \\ &= \mu\left[x \sum_{\substack{p=o,r \\ q=c,o}} \epsilon_p \left(\frac{1}{R_q^p}\right)^3 - \frac{3}{2}x^3 \sum_{\substack{p=o,r \\ q=c,o}} \epsilon_p \left(\frac{1}{R_q^p}\right)^5\right],\end{aligned}$$

$$\begin{aligned}A(x) &= \mu \sum_{\substack{p=o,r \\ q=c,o}} \epsilon_p \frac{\sin^2 \beta_q^p(x)}{R_q^p(x)} \\ &= \mu\left[x^2 \sum_{\substack{p=o,r \\ q=c,o}} \epsilon_p \left(\frac{1}{R_q^p}\right)^3 - \frac{3}{2}x^4 \sum_{\substack{p=o,r \\ q=c,o}} \epsilon_p \left(\frac{1}{R_q^p}\right)^5\right],\end{aligned}$$

$$\begin{aligned}F(x) &= \frac{-1}{R_i(x)} + \mu \sum_{\substack{p=o,r \\ q=c,o}} \epsilon_p \frac{1}{R_q^p(x)} \\ &= \mu\left[-\frac{x^2}{2} \sum_{\substack{p=o,r \\ q=c,o}} \epsilon_p \left(\frac{1}{R_q^p}\right)^3 + \frac{x^4}{2} \sum_{\substack{p=o,r \\ q=c,o}} \epsilon_p \left(\frac{1}{R_q^p}\right)^5\right].\end{aligned} \tag{15}$$

where S, C, and A denote the spherical, coma, and astigmatism aberrations, respectively, and F denotes the field curvature. Also, the parameter $\epsilon_p \equiv 1$ for $p = o$, and $\epsilon_p \equiv -1$ for $p = r$. It is apparent from Eq. (15) that the first and the second orders of the aberrations $C(x)$, $A(x)$, and $F(x)$ can be canceled simultaneously if the following conditions are fulfilled

$$\sum_{\substack{p=o,r \\ j=c,s}} \epsilon_p \left(\frac{1}{R_j^p}\right)^3 = \sum_{\substack{p=o,r \\ j=c,s}} \epsilon_p \left(\frac{1}{R_j^p}\right)^5 = 0. \tag{16}$$

The dominant aberration of $\mathcal{H}_4$ now becomes $S(x) = 1/R_4^3$, but because the diameter of the eye d_{eye} is typically much smaller than the focal length R_4, this spherical aberration is negligible[4] and its contribution to the overall spot size is small. The relations that describe the relevant parameters of the interim holograms are given in Eqs. (3) and (16), which comprise a set of four equations with six variables. There is an infinite number of solutions to this set, and the exact solution can be chosen from various considerations such as an increase in the diffraction efficiency of $\mathcal{H}_4$ or simplification of the recording procedure.

4. Design Illustration and Experimental Results

Our design procedure is illustrated here for a HDVD having the following parameters:

$$R_4 = 87.8 \text{ mm}, \quad R_H = 32.3 \text{ mm}, \quad d_{eye} = 4 \text{ mm},$$
$$\bar{\beta}_c^g = \bar{\beta}_c = 48°, \quad R_{eye} = 40 \text{ mm}, \quad D_h = 24 \text{ mm},$$
$$T_h = 3 \text{ mm}, \quad \nu = 1.51, \quad \lambda_o = 457.9 \text{ nm},$$
$$\lambda_c = 632.8 \text{ nm} \Rightarrow \mu = 1.38, \tag{17}$$

where D_h is the lateral distance between the center of the two holograms and T_h is the thickness of the substrate. In order to illuminate $\mathcal{H}_4(0)$ with the full width of the image wave of $\mathcal{H}_g(o)$, we must fulfill the relation $2nT_h \tan \bar{\beta}_c = D_h$, where n is an integer number. In our case the desired relation is fulfilled with $n = 7$.

The performance of the doublet was checked over a FOV of ±6°, so the minimal angle inside the substrate is

$$\nu \sin \bar{\beta}_c^{min}(x) = \nu \sin \bar{\beta}_c - \sin(6°) \Rightarrow \sin \bar{\beta}_c^{min}(x) = 42.37°. \tag{18}$$

Substituting Eq. (18) into Eq. (1) yields

$$1.5 > \sin \bar{\beta}_c^{min}(x) = 1.01 > 1. \tag{19}$$

Inequality (19) demonstrates that the necessary condition for total internal reflection is fulfilled over the entire FOV of ±6°. Inserting the values of Eqs. (17) into Eqs. (2) and (15) yields the parameters for $\mathcal{H}_1^o$ and $\mathcal{H}_1^r$:

$$R_o^o = 170.26 \text{ mm}, \quad \beta_c^o = 78°, \quad R_c^o = -1905 \text{ mm},$$
$$R_o^r = -126.7 \text{ mm}, \quad \beta_c^r = -9.5°, \quad R_c^r = 200 \text{ mm}. \tag{20}$$

With the parameters of Eqs. (20) a simulation was performed in order to calculate the spot sizes for a corrected HDVD denoted by $\mathcal{H}_1$ and for a noncorrected HDVD (which was recorded with spherical waves) denoted by $\mathcal{H}_2$. Figure 3 shows the calculated spot sizes for a FOV of ±6°. It is evident from the results that there is a significant improvement for $\mathcal{H}_1$. The spot sizes for $\mathcal{H}_1$ over the entire FOV are much smaller than 33 μm, which is the diffraction-limited spot size, whereas those for $\mathcal{H}_2$ reach more than 80 μm.

To verify our design, we recorded the interim holograms $\mathcal{H}^o$ and $\mathcal{H}^r$. We transferred the exact image wave fronts from the interim holograms into the recording plane of the final element $\mathcal{H}_2$ in the HDVD $\mathcal{H}_1$ with the help of an intermediate hologram arrangement.[4] On the same substrate, but spatially displaced from $\mathcal{H}_4$, we recorded the simple grating $\mathcal{H}_g$. The recording was done in AGFA 8E56 photographic plates. The recording wavelength was 457.9 nm, derived from an argon laser. We then tested the HDVD $\mathcal{H}_1$ by introducing plane waves from a rotating mirror at the location of the eye. Figure 4 shows the experimental results for a FOV of ±6°. These results illustrate that $\mathcal{H}_1$ indeed has an essentially diffraction-limited performance.

To illustrate the improved chromatic sensitivity of the HDVD, we calculated the maximum lateral dispersion as a function of the output wavelength shift $\Delta\lambda_c$ for two different visor displays. One was composed of a single holographic element,[3] and the other was composed of a HDVD with planar optics. The re-

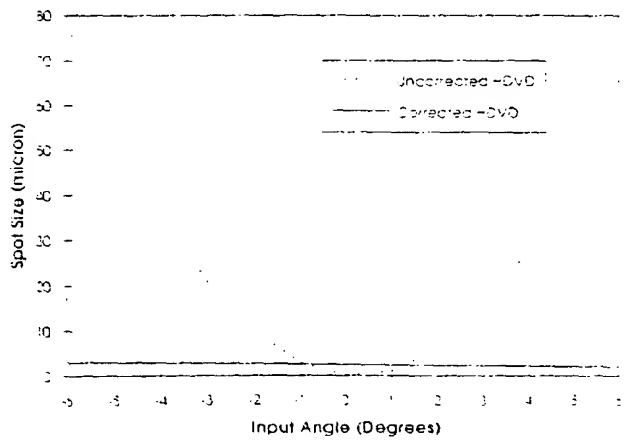

Fig. 3. Calculated spot sizes for the corrected HDVD $\mathcal{H}_1$ (solid curve) and the noncorrected HDVD $\mathcal{H}_2$ (dashed curve) covering a FOV of ±6°.

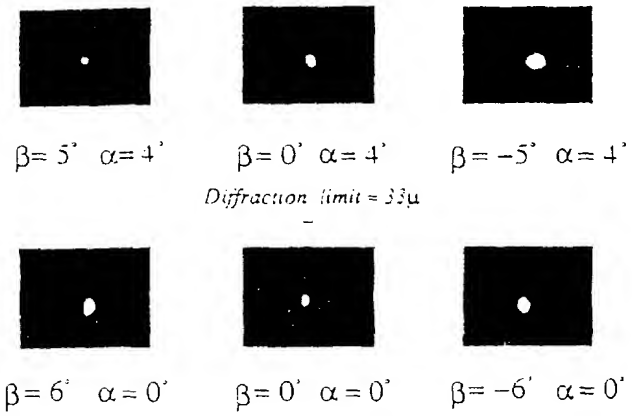

Fig. 4. Experimental spot sizes in the focal plane for the corrected HDVD.

sults are presented in Fig. 5. As shown, inside a bandwidth of ±2 nm, the lateral dispersion for the visor display with the HDVD is smaller than the diffraction-limited spot size. Moreover, this lateral dispersion is better by a factor of 7 than the lateral dispersion for the visor display with the single HOE.

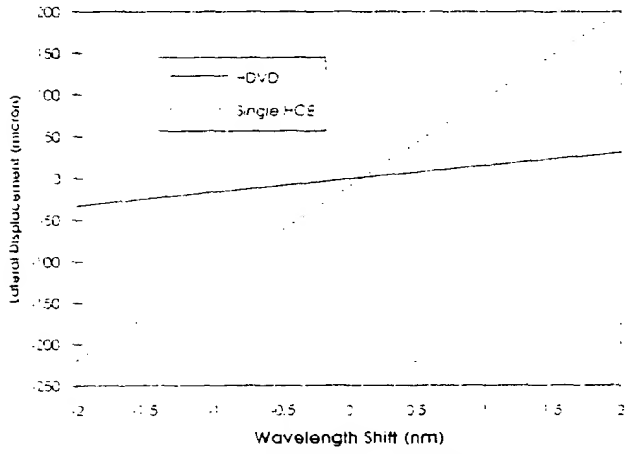

Fig. 5. Chromatic variation in the lateral focal position.

5. Concluding Remarks

We have demonstrated a method for designing and recording a compact-mode holographic doublet visor display. It is capable of providing excellent imaging and relatively low chromatic dispersion over a wide FOV. Both the design and the recording procedures are fairly simple; there is no need to resort to complicated computer-generated holograms nor to aspherical lenses. This design and these recording procedures need not be confined to visor-display applications but can be exploited in others, such as heads-up displays for aircrafts and cars. For all these applications, investigations are still needed and are currently ongoing in our laboratories to ensure that light efficiencies, noise levels, and other relevant parameters are optimized.

This work was supported in part by the Levin Fund.

References

1. R. C. Fairchild and J. R. Fienup, "Computer-originated aspheric holographic optical element," Opt. Eng. **21**, 133–140 (1982).
2. K. A. Winick and J. R. Fienup, "Optimum holographic elements with nonspherical wave front," J. Opt. Soc. Am. **73**, 208–217 (1983).
3. J. Kedmi and A. A. Friesem, "Optimal holographic Fourier-transform lens," Appl. Opt. **23**, 4015–4019 (1984).
4. Y. Amitai and A. A. Friesem, "Design of holographic optical elements by using recursive technique," J. Opt. Soc. Am. A **5**, 702–712 (1988).
5. H. P. Herzig, "Holographic optical elements for semiconductor lasers," Opt. Commun. **58**, 144–148 (1986).
6. H. Chen, R. R. Hershey, and E. Leith, "Design of a holographic lens for the infrared," Appl. Opt. **26**, 1983–1988 (1989).
7. Y. Amitai, A. A. Friesem, and V. Weiss, "Holographic elements with high efficiency and low aberrations for helmet displays," Appl. Opt. **28**, 3405–3416 (1989).
8. R. K. Kostuk, Y. T. Huang, D. Hetherington, and M. Kato, "Reducing alignment and chromatic sensitivity of holographic optical interconnects with substrate-mode holograms," Appl. Opt. **28**, 4939–4944 (1991).
9. J. Jahns and S. Walker, "Imaging with planar optical systems," Opt. Commun. **76**, 313–317 (1989).
10. Y. Amitai and J. W. Goodman, "Design of substrate-mode holographic interconnects with different recording and readout wavelengths," Appl. Opt. **30**, 2376–2381 (1991).
11. E. Hasman and A. A. Friesem, "Analytic optimization of holographic optical elements," J. Opt. Soc. Am. A **6**, 62–69 (1989).